Vol. 40 (2009) ACTA PHYSICA POLONICA B No 3

SPECTROSCOPY OF NEUTRON-RICH NUCLEI WITH THE CLARA-PRISMA SETUP*

E. Farnea

INFN Sezione di Padova, Italy

on behalf of

the CLARA-PRISMA and the AGATA Collaborations

(Received December 12, 2008)

The CLARA-PRISMA setup, composed of an array of 25 Clover detectors placed at the target position of the magnetic spectrometer PRISMA, has recently concluded its campaign to study the structure of moderately neutron-rich nuclei. In this contribution, results obtained in the vicinity of the doubly-magic nucleus ^{48}Ca are presented, together with results obtained for the heavy iron isotopes. The perspectives offered by the forthcoming operation of the AGATA Demonstrator Array coupled to PRISMA are also discussed.

PACS numbers: 29.30.Aj, 29.30.Kv, 25.70.Hi

1. Introduction

Since several years, the use of binary reactions, quasi-elastic (multinucleon transfer) or deep inelastic reactions has become a well-established technique to study the structure of moderately neutron-rich nuclei. Recent cross section measurements, for selected multinucleon transfer reactions, with neutron-rich stable targets have shown the potentiality of this reaction mechanisms to populate neutron-rich nuclei with sizeable cross section values [1], such that in-beam γ-spectroscopy of these nuclei is feasible using the modern γ-ray arrays such as GASP, Gammasphere or Euroball. The binary nature of these reactions poses several experimental problems. On one hand, the γ–γ coincidences between unknown transitions from the neutron-rich nucleus and known ones from the reaction partner can be used to deduce the decay scheme of the neutron-rich nucleus, as shown for instance in [2] and in

* Presented at the Zakopane Conference on Nuclear Physics, September 1–7, 2008, Zakopane, Poland.

subsequent experiments. On the other hand, the reaction partner might not be unique due to neutron evaporation following the multinucleon transfer process, especially in neutron-rich nuclei. This increases the difficulty of the identification, and in addition it is almost impossible to provide firm identification for neutron-rich nuclei having an unknown binary partner. The experimental approach pursued in the present work relies instead on the possibility to assign the γ-transitions to the corresponding reaction product through the use of γ-ion coincidences. In a joint effort, γ-spectroscopy and reaction mechanisms groups belonging to INFN, in collaboration with several European institutes, have developed a new setup by coupling the array of Euroball Clover detectors CLARA [3] to the existing large acceptance magnetic spectrometer PRISMA [4, 5]. The optical design of PRISMA is very simple, consisting of a quadrupole singlet and of a dipole. No further optical elements correcting for aberrations are used, rather the trajectory of each ion is software reconstructed starting from the information provided by position-sensitive start and focal plane detectors. This way, a large solid angle acceptance (approximately 80 msr) is obtained, combined with mass resolution up to $\Delta A/A \approx 1/300$ and Z resolution $\Delta Z/Z \approx 1/60$. Within the limitation of the Z and mass resolutions, PRISMA allows for the unambiguous identification of the reaction products as well as for the full vector velocity of each ion. CLARA is an array of 25 composite EUROBALL CLOVER detectors [6] with Compton-suppression shield, placed at the target position of PRISMA. The performance of CLARA for $E_\gamma = 1.3$ MeV are the following: photopeak efficiency $\approx 3\%$, peak/total ratio $\approx 45\%$ and energy resolution $\approx 0.6\%$ for $v/c = 10\%$. The latter value is obtained, despite the broad range of product velocities in typical multinucleon transfer reaction, thanks to the excellent event-by-event definition of the recoil velocity provided by PRISMA.

2. Spectroscopic studies of medium-mass neutron-rich nuclei

One of the most critical ingredients for determining the properties of a nucleus from a given effective interaction, is the overall number of nucleons and the ratio N/Z of neutrons to protons. Intuitively, since the spin–orbit interaction is essentially a surface phenomenon, it is expected to be reduced in nuclei with a diffused surface, such as nuclei with a large neutron excess. This causes a migration of the high-l orbitals, with a large impact on the shell structure of nuclei very far from stability [7–9], close to the driplines, beyond the species reachable with the technique used in the present work. Other mechanisms driving the evolution of the shell structure in going from stable to exotic nuclei have been recently invoked. These effects, which are effective also in moderately neutron-rich species, can be related to the effect of the tensor part of the nucleon–nucleon interaction [10, 11], which is one of the most direct manifestations of the meson-exchange origin of the nucleon–nucleon interaction. The tensor interaction results ultimately in attraction or repulsion between proton and neutron orbitals. The effect becomes particularly visible when moving away from the valley of stability. In such cases the removal of nucleons from one orbital significantly modifies the proton–neutron monopole interaction, which in turn, affects the effective single-particle energies, hence the shell structure.

A neutron-rich region where the shell evolution is apparent is the one bounded by $N = 28$–50 and $Z = 20$–28. Spectroscopic studies of the region proved that a new subshell closure is indeed present at $N = 32$ [12], which is a good subshell closure for the neutron-rich calcium isotopes but is rapidly quenched when adding protons in the $1f_{7/2}$ orbital. This quenching is due to the strong spin-orbit $1f_{7/2} - 1f_{5/2}$ proton–neutron monopole interaction [11], reducing the spacing between the $\nu p_{3/2}$, $\nu p_{1/2}$ and the $\nu f_{5/2}$ single-particle orbitals. As a result, the $N = 32$ subshell gap practically disappears above the chromium isotopes. It should be remarked that some shell model calculations predict that also $N = 34$ should also be a good subshell closure for the calcium isotopes [13, 14], but not for larger Z values, again due to the $1f_{7/2} - 1f_{5/2}$ proton–neutron monopole interaction. So far, this prediction has not been verified experimentally.

Moving towards the middle of this nuclear region, according to the theoretical predictions [15], nuclear deformation sets in and the subshell closure at $N = 40$ disappears. This effect is origined by the coupling of neutrons excited to the *sdg* shell and of protons in the *pf* shell, which can occur when the proton $1f_{7/2}$ shell is not completely filled. The calculations predict that the removal of two or four protons from the spherical ^{68}Ni drives the $N = 40$ nuclei ^{66}Fe and ^{64}Cr into prolate shapes generating a new region of deformation [15].

2.1. The ^{48}Ca region

Experimental studies of nuclei in the ^{48}Ca region have been carried out to investigate the possible impact of the new phenomena in the structure of the region. In the present work, nuclei in the vicinity of ^{48}Ca were populated through the ^{48}Ca(330 MeV)+^{238}U reaction, performed at the Tandem-ALPI accelerator facility of the Laboratori Nazionali di Legnaro. Clean γ-ion coincidences were collected using the CLARA-PRISMA setup, providing firm assignment of several new transitions in nuclei such as ^{51}Ca, ^{52}Sc, ^{47}K, ^{48}K. This was instrumental in re-analyzing a previous Gammasphere thick target experiment, performed at the ATLAS accelerator of the Argonne National Laboratory with the same reaction. Using γ–γ coincidences and exploiting the firm identification provided by the CLARA-PRISMA data it was possible to construct complex level schemes for several isotopes [16].

The structure of the $N = 31$ isotones ^{51}Ca, ^{52}Sc, ^{53}Ti is generally well reproduced by shell model calculations using the GXPF1A interactions, with the notable exception of the levels involving the occupancy of the $\nu f_{5/2}$ orbital, namely a $9/2^-$ level in ^{51}Ca ($\nu p^2_{3/2} f_{5/2}$), a 8^+ level in ^{52}Sc ($\pi f_{7/2} \nu p^2_{3/2} f_{5/2}$) and a $21/2^-$ level in ^{53}Ti ($\pi f^2_{7/2} \nu p^2_{3/2} f_{5/2}$), shown in Fig. 1. The difference between the experimental and the calculated energy of these levels increases with the decreasing proton number, namely with the increasing N/Z ratio.

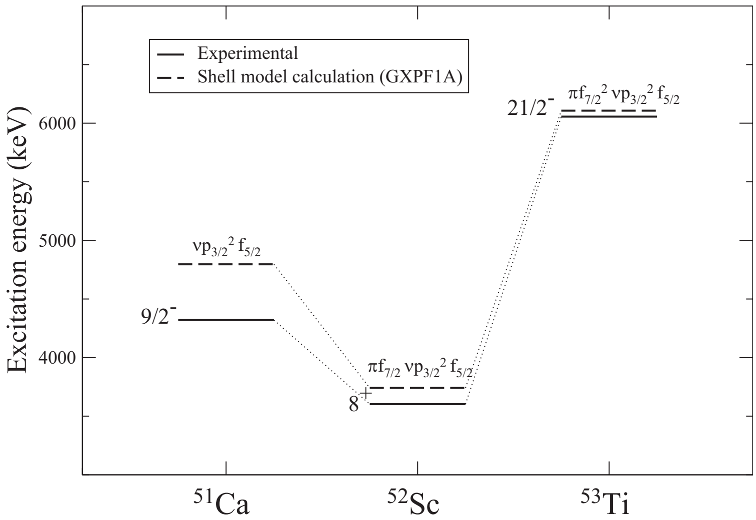

Fig. 1. Comparison between the experimental and the calculated energies of levels involving the occupancy of the $\nu f_{5/2}$ orbital in the $N = 31$ isotones ^{51}Ca, ^{52}Sc, ^{53}Ti. The GXPF1 interaction was assumed in the shell-model calculations. See text for details.

This suggests that the $\nu p_{1/2} - \nu f_{5/2}$ energy difference might be somewhat smaller than the predictions of the GXPF1A interaction [13, 14]. This can be explained, as mentioned earlier, by the migration in energy of the $\nu f_{5/2}$ single-particle state due to the strong proton $\pi f_{7/2}$ -neutron $\nu f_{5/2}$ interaction causing a decrease in energy of the $\nu f_{5/2}$ single-particle orbital with respect to the $\nu p_{3/2}$ and $\nu p_{1/2}$ levels as protons are added to the $\pi f_{7/2}$ shell [11].

Further insight on the structure of the moderately neutron-rich nuclei around ^{48}Ca was gained through a lifetime measurement performed with CLARA-PRISMA, using the Recoil Distance Doppler Shift Method with a differential plunger. In this case, nuclei of interest were populated via the ^{48}Ca(330 MeV)+^{208}Pb multinucleon transfer reaction. The results from this measurement are presented elsewhere [17].

2.2. The neutron-rich iron isotopes

The structure of the neutron-rich iron and chromium isotopes was studied through two measurements performed at the Tandem-ALPI accelerator facility of the Laboratori Nazionali di Legnaro with the CLARA-PRISMA setup. In the first experiment, the nuclei of interest were populated via the ^{64}Ni(400 MeV)+^{238}U reaction. It was possible to collect valuable information on the even neutron-rich iron isotopes up to ^{66}Fe [18], although for this last nucleus only one γ-ray transition could be safely identified. A second measurement was performed in order to enhance the population of the heavy iron isotopes, using the ^{70}Zn(460 MeV)+^{238}U reaction [19]. The comparison of the spectra for ^{66}Fe obtained in the two experiments, shown in Fig. 2, clearly proves that in the second measurement the population cross section for the heavy iron isotopes was greatly enhanced.

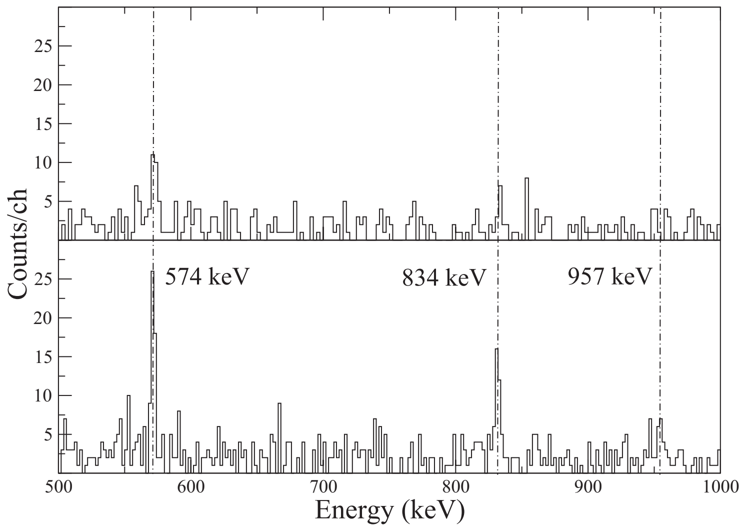

Fig. 2. Spectra in coincidence with ^{66}Fe isotopes detected in PRISMA, respectively for the ^{64}Ni(400 MeV)+^{238}U (top) and the ^{70}Zn(460 MeV)+^{238}U reaction (bottom). In the former case, only the $2^+ \to 0^+$ ground-state transition can be firmly assigned, while in the latter case also the $6^+ \to 4^+$ and the $4^+ \to 2^+$ can be identified, proving that the population of ^{66}Fe is enhanced.

The decay schemes for the even neutron-rich iron isotopes studied in this work is presented in Fig. 3 together with the result from large-scale shell-model calculations. The effective interaction used is called *fpg* and is described in Ref. [20]. An inert core of ^{48}Ca was considered, with a valence space including the whole *fp* shell for the protons and the $p_{3/2}$, $f_{5/2}$, $p_{1/2}$, and $g_{9/2}$ orbitals for the neutrons [19]. Suitable truncations were imposed to limit the dimensions of the matrices.

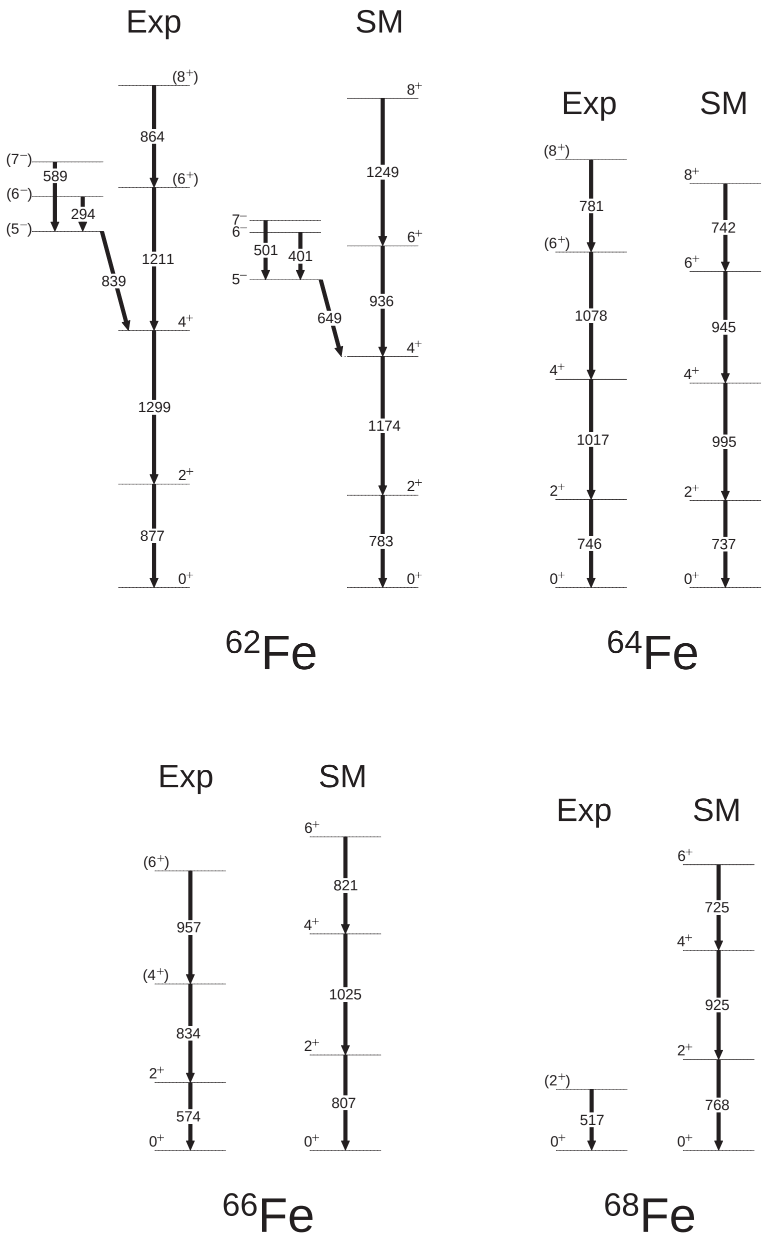

Fig. 3. Decay schemes for the even iron isotopes ^{62,64,66,68}Fe obtained during the CLARA-PRISMA campaign, compared with the results from large-scale shell-model calculations performed with a *fpg* interaction [18, 19]. See text for details.

Iron isotopes evolve toward more collective structures when approaching $N = 40$. Inspection of Fig. 2 shows in fact that the excitation energy of the 2^+ state (usually considered a first fingerprint of nuclear collectivity) decreases with increasing neutron number in the even-A iron isotopes. In particular, at $N = 40$ (that for nickel isotopes acts as a subshell closure [21]), the drop in the 2^+ excitation energy is large, which suggests increasing collectivity. This can be understood in terms of a decrease of the energy gap between the *fp* shell and the intruder $g_{9/2}$ orbital when the $1f_{7/2}$ proton shell is not completely filled and more neutrons are occupying the upper shell [15]. The fact that the $f_{7/2}$ shell is not fully occupied weakens both the effect of the attractive monopole tensor interaction with the neutrons in the $f_{5/2}$ orbital and the repulsion with those in the the neutron $g_{9/2}$ orbital.

The theoretical description of the even-A isotopes ^{62,64}Fe (Fig. 2) is quite satisfactory, although the calculated level schemes are more compressed than the experimental ones. Furthermore, in the case of ^{66}Fe, the excitation energy of the 2^+ state is predicted too high. The dramatic decrease of the energy of the 2^+ state in this nucleus suggests that the $d_{5/2}$ orbital has to be considered as well, as suggested in Ref. [19].

3. Future perspectives: the AGATA Demonstrator Array

The goal of the AGATA project is the construction of an array of high-purity germanium detectors with very high photopeak efficiency (larger that 40%) and peak-to-total ratio (larger than 50%) under a wide range of experimental conditions. Such values can only be achieved by operating the HPGe detectors in position-sensitive mode so as to be able to reconstruct the scattering path of each photon inside the crystals (this process is known as *γ-ray tracking*).

The information on the interaction points within the detectors is extracted by comparing the observed signal shapes with "reference" signals corresponding to interactions taking place in known locations. This process, known as *pulse shape analysis*, requires using electrically-segmented crystals and digital electronics. In the initial phase of the AGATA project, a subset of the array, known as the AGATA Demonstrator Array, will be built to prove that the pulse shape analysis and the γ-ray tracking data processing can actually be performed in real time, which is a key issue of the project. The AGATA Demonstrator Array will be composed of 15 crystals, arranged into 5 triple clusters, and will be first installed at the Laboratori Nazionali di Legnaro, where it will replace the CLARA array at the target position of PRISMA. The installation of the Demonstrator Array is in progress, and it is expected to start operation in the first half of 2009. Following the commissioning and the "demonstration" phase, a one-year campaign of measurements is planned which could extend up to the end of 2010. Several letters of interest were already submitted to the LNL PAC.

The expected performance of the AGATA Demonstrator Array in terms of photopeak efficiency will be comparable to the existing arrays, with values ranging from 3% to 7% depending on the distance from the target at which the detectors will be placed. The major improvement will actually be the much better quality of the spectra, resulting from the 5 mm FWHM position resolution expected from the pulse shape analysis process. Realistic Monte Carlo simulations of the full AGATA+PRISMA setup show that the effective energy resolution of the AGATA Demonstrator will be very close to the limiting intrinsic resolution value. For instance, the simulated data shown in Fig. 4 refer to the case of ^{90}Zr nuclei with an average energy of 350 MeV, with a Gaussian energy distribution having FWHM = 100 MeV. Each ion was emitting a single photon of 1 MeV energy. Doppler correction

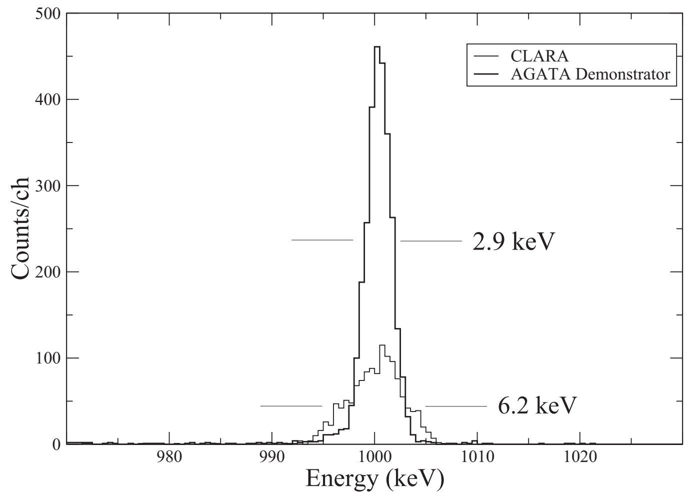

Fig. 4. Comparison between simulated data for the CLARA-PRISMA (narrow line) and for the AGATA Demonstrator + PRISMA setups (thick line). In both cases, ^{90}Zr nuclei with an average energy of 350 MeV were assumed, with a Gaussian energy distribution having FWHM = 100 MeV. Each ion was emitting a single photon of 1 MeV energy. Doppler correction was performed using the full information from PRISMA.

was performed using the full information from PRISMA. The resulting peak FWHM is 6.2 keV and 2.9 keV respectively for CLARA and the AGATA Demonstrator, the latter value being less than 1 keV larger than the intrinsic detector resolution. This will be a major advantage for all of the planned experiments, and especially for further lifetime measurements with the differential plunger. In this case, the combination of larger photopeak efficiency and better effective energy resolution will provide an improvement in sensitivity of over an order of magnitude compared to the CLARA array.

The author is indebted to all of the colleagues that contributed to the operation of CLARA-PRISMA and in particular to the technical staff (P. Cocconi, M. Giacchini, R. Isocrate, D. Rosso) for their skillful help. Valuable discussions with several colleagues who shared their data for this and many other presentations is gratefully acknowledged here, in particular the author would like to mention R. Broda, R. Chapman, B. Fornal, A. Gadea, S.M. Lenzi and S. Lunardi. This work has been partially supported by the European Commission through I3-EURONS (contract no. RII3-CT-2004-506065).

REFERENCES

[1] L. Corradi *et al.*, *Phys. Rev.* **C63**, 021601 (2001), and references therein.
[2] R. Broda *et al.*, *Phys. Lett.* **B251**, 245 (1990).
[3] A. Gadea *et al.*, *Eur. Phys. J.* **A20**, 193 (2004).
[4] A.M. Stefanini *et al.*, *Nucl. Phys.* **A701**, 109c (2002).
[5] A. Latina *et al.*, *Nucl. Phys.* **A734**, E1 (2004).
[6] G. Duchêne *et al.*, *Nucl. Instrum. Methods* **A432**, 90 (1999).
[7] J. Dobaczewski *et al.*, *Phys. Scr.* **T56**, 15 (1995).
[8] R.C. Nayak, *Phys. Rev.* **C60**, 064305 (1999).
[9] N. Fukunishi *et al.*, *Phys. Lett.* **B296**, 279 (1992).
[10] T. Otsuka *et al.*, *Phys. Rev. Lett.* **87**, 082502 (2001).
[11] T. Otsuka *et al.*, *Phys. Rev. Lett.* **95**, 232502 (2005).
[12] J.I. Prisciandaro *et al.*, *Phys. Lett.* **B510**, 17 (2001).
[13] M. Honma *et al.*, *Eur. Phys. J.* **A25 s01**, 499 (2005).
[14] M. Honma *et al.*, *Phys. Rev.* **C65**, 061301(R) (2002).
[15] E. Caurier, F. Nowacki, A. Poves, *Eur. Phys. J.* **A15**, 145 (2002).
[16] B. Fornal *et al.*, *Phys. Rev.* **C77**, 014304 (2008).
[17] D. Mengoni *et al.*, *Acta Phys. Pol. B* **40**, 485 (2009) these proceedings.
[18] S. Lunardi *et al.*, *Phys. Rev.* **C76**, 034303 (2007).
[19] S.M. Lenzi *et al.*, Report INFN-LNL-222(2008), 15 (2008).
[20] O. Sorlin *et al.*, *Phys. Rev. Lett.* **88**, 092501 (2002).
[21] R. Broda *et al.*, *Phys. Rev. Lett.* **74**, 868 (1995).